

**This is the final draft of the contribution published as:**

Ghanem, N., Stanley, C.E., Harms, H., Chatzinotas, A., Wick, L.Y. (2019):  
Mycelial effects on phage retention during transport in a microfluidic platform  
*Environ. Sci. Technol.* **53** (20), 11755 - 11763

**The publisher's version is available at:**

<https://doi.org/10.1021/acs.est.9b03502>

1 **MYCELIAL EFFECTS ON PHAGE RETENTION DURING TRANSPORT IN A**  
2 **MICROFLUIDIC PLATFORM**

3

4 Nawras Ghanem<sup>1</sup>, Claire E. Stanley<sup>2</sup>, Hauke Harms<sup>1,3</sup>, Antonis Chatzinotas<sup>1,3</sup> and Lukas Y. Wick<sup>1\*</sup>

5

6

7

8 <sup>1</sup>Helmholtz Centre for Environmental Research - UFZ, Department of Environmental Microbiology,  
9 Permoserstraße 15, 04318 Leipzig, Germany.

10 <sup>2</sup>Agroecology and Environment Research Division, Agroscope, Reckenholzstrasse 191, 8046 Zurich,  
11 Switzerland

12 <sup>3</sup>German Centre for Integrative Biodiversity Research (iDiv) Halle-Jena-Leipzig, Deutscher Platz 5e,  
13 04103 Leipzig, Germany

14

15

16

17

18 Running title: Transport of tracer phages along mycelia

19

20

21 Intended for: Environmental Science and Technology

22

23

24

25

26 \* Corresponding author: Helmholtz Centre for Environmental Research - UFZ. Department of  
27 Environmental Microbiology; Permoserstrasse 15; 04318 Leipzig, Germany. Phone: +49 341 235  
28 1316, fax: +49 341 235 45 1316, e-mail: [lukas.wick@ufz.de](mailto:lukas.wick@ufz.de).

29 **ABSTRACT**

30 Phages (i.e. viruses that infect bacteria) have been considered as good tracers for the hydrological  
31 transport of colloids and (pathogenic) viruses. Little, however, is known about interactions of phages  
32 with (fungal) mycelia as the prevalent soil microbial biomass. Forming extensive and dense  
33 networks, mycelia provide significant surfaces for phage-hyphal interactions. Here, we for the first  
34 time quantified the mycelial retention of phages in a microfluidic platform that allowed for defined  
35 fluid exchange around hyphae. Two common lytic tracer phages (*Escherichia coli* phage T4 and  
36 marine phage PSA-HS2) and two mycelia of differing surface properties (*Coprionopsis cinerea*,  
37 *Pythium ultimum*) were employed. Phage-hyphal interaction energies were approximated by the  
38 extended Derjaguin-Landau-Verwey-Overbeek (XDLVO) approach of colloidal interaction. Our data  
39 show initial hyphal retention of phages of up to  $\approx 4 \times 10^7$  PFU mm<sup>-2</sup> ( $\approx 2550$  PFU mm<sup>-2</sup> s<sup>-1</sup>) with a  
40 retention efficiency depending on the hyphal and, to a lesser extent, the phage surface properties.  
41 Experimental data were supported by XDLVO calculations, which revealed the highest attractive  
42 forces for the interaction between hydrophobic T4 phages and hydrophobic *C. cinerea* surfaces. Our  
43 data suggest that mycelia may be relevant for the retention of phages in the subsurface and need to be  
44 considered in subsurface phage tracer studies. Mycelia-phage interactions may further be exploited  
45 for the development of novel strategies to reduce or hinder the transport of undesirable (bio-)colloidal  
46 entities in environmental filter-systems.

47

48 **KEYWORDS:** marine phages, tracer, hyphae, microfluidic platform, transport, mycelia

49

50

51

52

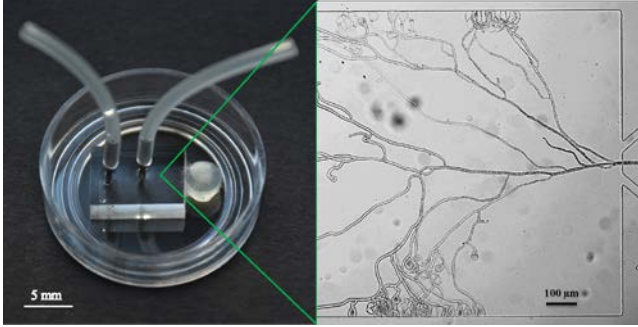
53

54

55

56  
57  
58  
59  
60  
61

**TOC / ABSTRACT ART**



62  
63  
64  
65

## 66 INTRODUCTION

67 Previous work has highlighted the relevance of phages (i.e. viruses that infect bacteria)<sup>1,2</sup> as  
68 promising tracers for fecal contamination or for the evaluation of colloidal and water transport.<sup>3,4,5</sup>  
69 Although phage tracers have significantly improved our understanding of water and colloid  
70 movement in aquifers<sup>6</sup>, information on the transport of phage tracers in the complex soil subsurface  
71 is still limited, yet highly needed. For example, accurate descriptions of microbial (colloid) transport  
72 and soil-related transport drivers are needed to assess the risk of pathogen contamination to drinking  
73 water supplies or to develop control strategies and treatment options. Although still rarely applied,  
74 marine tracer phages hold much promise as tracers in subsurface ecosystems, as they and their hosts  
75 are absent in terrestrial ecosystems. Typically, up to  $10^{15}$  phages ( $\sim 1$  g) can be applied and phage  
76 concentrations of  $< 10$  phages  $\text{mL}^{-1}$  of recovered water can be detected<sup>7</sup> by specific interactions with  
77 their host bacteria using plaque forming unit (PFU) assays.<sup>7,8,9,10</sup> Subsurface transport of phages (and  
78 other viruses) is driven by environmental factors, phage type and phage interaction with  
79 autochthonous soil microorganisms.<sup>11</sup> Environmental factors included soil type and texture,<sup>12,13,14,15</sup>  
80 electrolyte composition<sup>16,17</sup> or the degree of water saturation in soil.<sup>11,18,19</sup> Other research assessed  
81 the influence of virus characteristics such as the effect of the isoelectric point,<sup>20</sup> combinations of size  
82 and isoelectric point<sup>21</sup> or the morphology of phages and other viruses.<sup>22</sup> While abiotic environmental  
83 drivers have been widely studied, insufficient knowledge exists concerning interactions of phages  
84 and viruses with non-host microbes (termed in the following as unspecific phage-microbe  
85 interactions). Such interactions may be of high importance for the transport and survival of  
86 pathogens in soil and the upper layer of the Earth's Critical Zone (CZ)<sup>23</sup>, i.e. the thin, living and  
87 permeable layer that connects the atmosphere with the geosphere. Research on unspecific phage-  
88 microbe interactions mainly evaluated the influence of sterile vs. non-sterile conditions on the fate of  
89 phages.<sup>24</sup> These studies suggest better survival of phages and other viruses in sterile rather than in  
90 non-sterile environments.<sup>24,25,26</sup> Other studies have highlighted the role of fungi as mediators for the

91 virulence of plant viruses.<sup>27,28,29</sup> To our knowledge, however, no literature exists on unspecific  
92 interactions of phages with hyphal surfaces or the effect of (fungal) mycelia on waterborne transport  
93 of phages.

94 Fungi occur in nearly every aerobic habitat, being important drivers of biogeochemical cycles<sup>30,31</sup>  
95 and fertility of soils. Being the major microbial biomass in soil, they typically develop a spatially  
96 extensive mycelium, which comprises up to 1000 m of hyphae per gram of dried soil.<sup>32,33</sup> Mycelia  
97 also provide ideal 'logistic networks' for bacterial evolution<sup>34,35,36</sup> as well as the transport of bacteria.  
98 Fungal growth is not restricted to saturated environments, as their hyphae are also able to breach air-  
99 water interfaces<sup>37</sup> and thereby connect different soil microenvironments.<sup>32</sup> Of central importance for  
100 possible phage transport is the observation that hyphae may change the physico-chemical properties  
101 of their surface<sup>38</sup> and hence, alter the water infiltration properties of soils through the production of  
102 large amounts of hydrophobic compounds in the outer cell wall.<sup>39</sup>

103 Here, we hypothesized that mycelia might retain phages, due to the physico-chemical interactions of  
104 phages with hyphal surfaces, and hence would influence waterborne phage transport. Using a well-  
105 controlled microfluidic platform, we quantified the effects of mycelia on phage retention and  
106 transport at the micrometer scale. The microfluidic platform allowed single hyphae to be subjected to  
107 a defined concentration of phages and to quantify their interactions by comparing the in- and outflow  
108 concentrations of phages. Two lytic phages commonly used as tracers to follow pathogen  
109 contamination (*E. coli* T4 phage) or colloidal particle transport<sup>22</sup> (marine phage PSA-HS2) were used  
110 as models. The phages belong to different virus families<sup>40,41</sup> and vary in their morphology and  
111 physico-chemical surface properties. Two filamentous soil organisms (*Coprinopsis cinerea* and  
112 *Pythium ultimum*) of varying surface hydrophobicity were also implemented. Experimental  
113 observations were accompanied by the extended Derjaguin-Landau-Verwey-Overbeek approach  
114 (XDLVO) of colloidal interaction that describes the forces between charged surfaces interacting in a

115 liquid medium. Our findings suggest that the mycosphere may significantly influence the transport  
116 and fate of phages and phage tracers.

117

## 118 **MATERIALS AND METHODS**

### 119 **Organisms and culture conditions**

120 Two well-characterized lytic tracer phages were studied (Table 1). The T4 coliphage (T4)<sup>42</sup> and its  
121 host *E. coli* (Migula 1895)<sup>43</sup> were purchased from Deutsche Sammlung von Mikroorganismen und  
122 Zellkulturen GmbH (DSMZ, Germany), while the marine phage PSA-HS2 and its host strain  
123 *Pseudoalteromonas* H13-15 were kindly provided by Dr. B. M. Duhaime (University of Michigan,  
124 USA).<sup>44</sup> The T4 coliphage (*Myoviridae*) and the PSA-HS2 (*Siphoviridae*) are of different  
125 morphology. Both phages were propagated, purified and counted as described previously.<sup>22</sup> *P.* H13-  
126 15 and *E. coli* were grown at room temperature using dilute (50%) 2216E medium<sup>45</sup> and Luria-  
127 Bertani (LB) medium<sup>46</sup>. Both phages were stored in SM buffer (100 mM NaCl, 8 mM MgSO<sub>4</sub> 7H<sub>2</sub>O,  
128 50 mM Tris-HCl, pH 7). Phages were quantified by a modified spotting plaque assay technique<sup>22</sup> by  
129 incubating phage host pairs overnight either at room temperature (RT, 25°C) (PSA-HS2) or at 37°C  
130 (T4 coliphage). The agaricomycete *C. cinerea* strain AmutBmut pMA412 (*C. cinerea*) and the  
131 oomycete *P. ultimum*<sup>32</sup> exhibit hyphal surfaces of varying hydrophobicity.<sup>38</sup> *C. cinerea* strain  
132 AmutBmut pMA412 constitutively expresses the red fluorescent protein dTomato.<sup>47</sup> *C. cinerea* and  
133 *P. ultimum* were cultivated on yeast-malt extract-glucose medium solidified with agar (YMG, Table  
134 S2) and Luria Bertani (LB) agar for three days at 30 °C and RT, respectively.<sup>47,48</sup>

### 135 **Stability and viability of phage suspensions**

136 Conditioned (i.e., cell-free) media were prepared by cultivating *C. cinerea* and *P. ultimum* in  
137 glucose-based liquid CCMM minimal<sup>47</sup> (Table S2) and LB media using a shaker incubator (SM-30,  
138 Edmund Bühler GmbH, Bodelshausen, Germany) at 150 rpm, at 30 °C for 9 d. Conditioned media  
139 were obtained by vacuum filtration of the mycelial suspensions using a glass frit (Schott pore 40,

140 DURAN® filter funnel, DWK Life Sciences, Wertheim, Germany) and subsequently stored at 4 °C.  
141 The stability (i.e. phage aggregation and infectivity) of phage suspensions was investigated in batch  
142 experiments at RT in 10 mL glass vials<sup>49</sup> containing 6 mL of phage suspensions ( $10^8$ - $10^9$  PFU mL<sup>-1</sup>)  
143 in conditioned media (Fig. S1). Experiments were performed in triplicate by exposing phages to the  
144 conditioned media for 0, 4 and 22 h and subsequently performing a PFU quantification (Fig. S1).  
145 The stability of the phage suspensions was calculated as the ratios of phage concentrations (Table 2).  
146 Similar experiments were performed using fresh media as controls (Fig. S2).

147

### 148 **Characterization of physico-chemical surface properties**

149 The contact angles of water  $\theta_w$ , formamide  $\theta_f$ , and methylene iodide  $\theta_{mi}$  were measured using a DSA  
150 100 drop-shape analysis system (Krüss GmbH, Hamburg, Germany). Briefly, mycelia of the  
151 organisms were cultivated for 2 - 3 days on a 0.45 µm-filter (NC 45, Cellulose Nitrate Membrane  
152 Whatman, Maidstone, Kent, United Kingdom) placed on the surface of LB (*P. ultimum*) or YMG  
153 agar plate (*C. cinerea*). Filters covered with fungi were removed and mounted on a microscope slide  
154 and the contact angles measured as detailed elsewhere.<sup>38,50</sup> The zeta-potential ( $\zeta$ ) for the mycelia of  
155 *C. cinerea* and *P. ultimum* were approximated from the electrophoretic mobility of hyphal elements  
156 measured by Doppler electrophoretic light scattering analysis (Zetamaster, Malvern Instruments,  
157 Malvern, UK). Mycelia of both organisms were cultivated for 3 days as described above. The  
158 biomass was then carefully scratched off the filter using a sterile spatula, suspended in 1 mL of SM  
159 buffer (100 mM, pH = 7) and homogenized using a micro-blender according to Potter-Elvehjem  
160 (Carl Roth GmbH + Co, Germany) prior to zeta potential measurement. The zeta potential of PSA-  
161 HS2 and T4 phage suspensions (SM buffer; 100 mM, pH = 7) was approximated as described  
162 earlier.<sup>22</sup>

163

### 164 **Phage transport experiments**

165 *Microfluidic device design and preparation*

166 Microfluidic devices were prepared as described in Stanley et al.<sup>47</sup> based on a channel architecture<sup>51</sup>  
167 that enables laminar flow conditions as a result of actively pumping solutions into the observation  
168 chamber (Figs. 1 & S3; cf. SI for detailed description).

169 *Incubation and visualization of mycelial growth structures*

170 Using a syringe (Injekt®Solo, 2 mL, B. Braun, Melsungen, Germany), the microfluidic devices were  
171 filled with either liquid LB medium for *P. ultimum* or glucose-based CCMM for *C. cinerea*. A small  
172 agar plug ( $\approx 6 \text{ mm}^2$ ) containing the fungal inoculum was placed next to the opening of the  
173 microfluidic channel (Fig. 1). The microfluidic devices were incubated for 24 h (*P. ultimum*) and 48  
174 h (*C. cinerea*) in a humid and dark environment to allow the mycelia to reach the end of the  
175 observation channel. Prior to the addition of the phages, the mycelial structure in the observation  
176 channel was determined using an AZ100M fluorescence microscope (Nikon, Düsseldorf, Germany)  
177 and Nikon NIS-Elements software. The surface area of the mycelia in the observation chamber  
178 ( $A_{\text{mycelia}}$ ) was approximated based on the total length of the mycelia in the observation chamber  
179 assuming hyphae to be tubes having a diameter of  $7 \pm 1 \text{ }\mu\text{m}$  (*C. cinerea*)<sup>47</sup> and  $10 \pm 3 \text{ }\mu\text{m}$  (*P.*  
180 *ultimum*) using ImageJ software<sup>52</sup> following a modified method described by Jenson et al. (Table 1).

181 <sup>53</sup>

182

183 *Quantification of phage Mass recovery*

184 The mass recovery ( $M$ ) was calculated as the ratio of the total number of phages in the effluent and  
185 the influent in a given time period ( $\Delta t$ ) as inferred from the difference of inlet ( $C_o$ ) and outlet ( $C_i$ )  
186 phage concentration as described by eq. 1

$$187 \quad M = \frac{\sum C_t \Delta t}{\sum C_o \Delta t} * 100 \quad (1)$$

188

189 *Quantification of phage retention*

190 Prior to addition of phage suspensions the microfluidic devices were carefully flushed with  $\approx 100 \mu\text{L}$   
 191 of SM buffer (100 mM, Ionic strength  $I_s \sim 360 \text{ mM}$ ) to replace the growth media. A syringe pump  
 192 (KD Scientific Inc., USA) loaded with Luer-lock syringes (Injekt@Solo, 2 mL, B. Braun,  
 193 Melsungen, Germany) was used to administer the phage suspension ( $\approx 3 \times 10^9 \text{ PFU mL}^{-1}$ ) into the  
 194 microfluidic channels at a volumetric flow rate of  $5 \mu\text{L h}^{-1}$  (average velocity:  $1.4 \times 10^{-4} \text{ m s}^{-1}$ ; time  
 195 for fluid to reach outflow: 43 s (cf. SI)). After 4 and 22 h at RT, samples from the inlet and the outlet  
 196 (i.e. aliquots from the well-mixed effluents after 0-4h (20  $\mu\text{L}$ ) and 4-22 h (90  $\mu\text{L}$ )) of triplicate  
 197 microfluidic devices containing mycelia were collected and the phages enumerated. Quadruplicate  
 198 experiments in mycelia-free microfluidic devices (control) revealed insignificant ( $< 2 \%$ ) losses of  
 199 phages in the devices and the tubing material (Fig. 2 & Table 2). The retention of phages to the  
 200 mycelial surface ( $R_p$ ) was calculated using eq. 2, with  $C_{t,\text{effluent}}$  and  $C_{t,\text{influent}}$  being the effluent and the  
 201 influent phage concentrations respectively,  $C_{t,\text{effluent, control}}$  the effluent phage concentrations in  
 202 mycelia-free controls,  $V_{t,\text{effluent}}$  the volume of effluent at sampling (20  $\mu\text{L}$  and 90  $\mu\text{L}$  after 4 h and 22  
 203 h, resp.) and  $A_{\text{mycelia}}$  the estimated surface area of the mycelia in  $\text{mm}^2$ .

$$204 \quad R_p = \frac{((C_{t,\text{influent}} - C_{t,\text{effluent}}) - (C_{t,\text{influent}} - C_{t,\text{effluent, control}})) * V_{t,\text{effluent}}}{A_{\text{mycelia}}} \quad (2)$$

205 The t-test (two-tailed distribution) was used to test for significance and to determine the level of  
 206 marginal significance (p-value).

207

### 208 **Calculations of phage-hyphal surface interaction energies**

209 The total interaction energy ( $G_{\text{XDLVO}}$ ) between phages and hyphal surfaces was predicted by the  
 210 extended Derjaguin-Landau-Verwey-Overbeek (XDLVO) theory of colloidal interactions.<sup>54</sup>  $G_{\text{XDLVO}}$   
 211 is the sum of the electrostatic repulsion ( $G_{\text{EDL}}$ ), the Lifshitz-van der Waals ( $G_{\text{LW}}$ ) and the acid-base  
 212 ( $G_{\text{AB}}$ ) interaction energy. While  $G_{\text{AB}}$  compares the energy status between attached and nonattached  
 213 situations,  $G_{\text{EDL}}$  and  $G_{\text{LW}}$  are functions of the separation distance,  $h$  (nm), between two surfaces<sup>55,56</sup>  
 214 (eq. 3):

215 
$$G_{\text{XDLVO}}(h) = G_{\text{AB}} + G_{\text{EDL}}(h) + G_{\text{LW}}(h) \quad (3)$$

216 Sphere-plate geometry was applied as phages are far smaller than the hyphal surfaces.<sup>57</sup>  $G_{\text{EDL}}$ ,  $G_{\text{LW}}$   
217 and  $G_{\text{AB}}$  were calculated as described previously.<sup>22</sup> Surface free energy calculations were based on  
218 measured contact angles of phages and fungi using water, formamide and methylene iodide as  
219 liquids (as described above) and the Young equation.<sup>58</sup> The Gibbs free energies (Table S1) and  
220 Hamaker constants were calculated using the surface free energies of studied phages and hyphal  
221 surfaces applying eq. S4 and eq. S11.

222

## 223 **RESULTS**

### 224 **Phage transport in microfluidic devices**

225 Interactions of phages with hyphal surfaces were investigated using a microfluidic platform under  
226 continuous flow conditions typical for subsurface water flows ( $1.2 \text{ m d}^{-1}$ )<sup>59</sup> (Fig. 1) by comparing the  
227 in- and effluent phage concentrations (Fig. 2; Table 2). Control experiments in the absence of  
228 mycelia (Table 2, Fig S2) revealed negligible (<2 %) differences between in- and effluent phage  
229 concentrations (Table 2). Water contact angle measurements revealed that *C. cinerea* ( $\theta_w = 131 \pm 2^\circ$ )  
230 and *P. ultimum* ( $\theta_w = 62 \pm 6^\circ$ ) were highly and moderately hydrophobic respectively. The T4 and  
231 PSA-HS2 phages were of similar size ( $\approx 200 \text{ nm}$ ) and surface charge ( $\zeta \approx -10 \text{ mV}$ ) yet differed in  
232 surface hydrophobicity (T4:  $\theta_w = 95^\circ$ ; PSA-HS2:  $\theta_w = 40^\circ$ ; Table 1).

233 In the presence of *P. ultimum*, differences between the PFU counts of PSA-HS2 and T4 phages in the  
234 in- and effluents of the microfluidic devices were small (i.e., < 4 %) and statistically not significant  
235 ( $p > 0.05$ ) at both time intervals (0 - 4 h and 4 - 22 h) (Fig. 2A & C and Table 2). The presence of  
236 highly hydrophobic *C. cinerea* hyphae, however, resulted in  $\approx 25 \%$  (PSA-HS2) and 90% (T4)  
237 reductions of the outflow concentration of the hydrophilic PSA-HS2 (Fig. 2B) and hydrophobic T4  
238 phages (Fig. 2D) after 4h ( $p \leq 0.05$ ). This corresponds to a mass recovery of  $M = 7 \%$  (T4) and  $M =$   
239  $77 \%$  (PSA-HS2) during the first 4 h of phage percolation (Table 2). Most likely due to blocking

240 effects of the hyphal collector (i.e., hyphal surface became progressively occluded), the retention of  
241 T4 phages was minimized as similar PFU counts for the effluents and controls were observed after  
242 22 h. As the hyphal density and morphology of the two mycelia differed (cf. Fig. 1C & D),  
243 micrographs of the hyphal structures in the observation chambers were taken, and the hyphal surface  
244 areas exposed to the percolating phages were estimated (Table 1). After 4 h, the calculated apparent  
245 (yet statistically not significant) retention of phages to the mycelial surface ( $R_P$ ) of *P. ultimum* was  $\approx$   
246  $2.3 \times 10^6$  PFU mm<sup>-2</sup> for T4 and  $4.3 \times 10^6$  PFU mm<sup>-2</sup> for phage PSA-HS2 (Table 2). The presence of  
247 the hydrophobic surface of *C. cinerea*, however, significantly retained both phages with  $R_P = 13.6 \times$   
248  $10^6$  PFU mm<sup>-2</sup> for PSA-HS2 and  $R_P = 36.7 \times 10^6$  PFU mm<sup>-2</sup> for T4 phages ( $p \leq 0.05$ ; Fig. 3). This  
249 results in estimated time-averaged deposition rates of 941 and 2550 PFU mm<sup>-2</sup> s<sup>-1</sup> for PSA-HS2 and  
250 T4, respectively (Table 2). Better phage retention by more hydrophobic mycelia of *C. cinerea* was  
251 also evidenced by smaller mass recovery of T4 and PSA-HS2 phages (Table 2).

252

### 253 **Effect of mycelial conditioned media on phage infectivity and colloidal stability**

254 As mycelial products may influence the stability and infectivity of phages, the effect of *P. ultimum*  
255 and *C. cinerea* conditioned media on the PFU counts of T4 and PSA-HS2 was quantified after  
256 exposing the phages to the conditioned media for 0, 4, and 22 h. After 4 h no statistically significant  
257 reduction on PSA-HS2 and T4 phage concentrations was observed (Table 2, Fig. S1). Similarly, no  
258 effects of the conditioned media on PSA-HS2 phage counts were observed after 22 h of exposure. By  
259 contrast, the highly hydrophobic T4 phages exhibited a slight, yet statistically significant ( $p \leq 0.05$ )  
260 decrease of  $\approx 14$  % PFU counts in the conditioned medium of *C. cinerea* yet not of *P. ultimum* ( $\approx 6$   
261 % decrease).

262

### 263 **Approximation of phage-hyphal surface interaction energies**

264 Phage-hyphal surface interaction energy ( $G_{\text{XDLVO}}$ ) profiles were calculated using the XDLVO theory  
265 (cf. eq. 3 & eq. S2) based on the sphere-plate model (Fig. 4, Table 1).<sup>57</sup> This model is well-accepted  
266 approach to estimate the interaction energies of a phage approaching a surface,<sup>57,60</sup> although phages  
267 are away from the uniform surfaces of colloidal particles. The  $G_{\text{XDLVO}}$  is characterized by three  
268 different interaction energies: the primary minimum ( $\Phi_{\text{min1}}$ ) as the deep energy at short separation  
269 distance  $h$  from the sorbent surface, the secondary minimum ( $\Phi_{\text{min2}}$ ) as the shallow energy at larger  
270 distances allowing for reversible phage adhesion, and the maximum energy barrier (i.e. the energy  
271 the phages need to overcome to get irreversibly attached at the  $\Phi_{\text{min1}}$ ) ( $\Phi_{\text{max1}}$ ).<sup>61,62</sup> For the given  
272 experimental conditions, the  $G_{\text{XDLVO}}$  profiles predicted either no ( $\Phi_{\text{max1}}$ : no to be calculated) or low  
273 ( $\Phi_{\text{max1}} = 4.7 \times 10^{-3} \text{ k}_B\text{T}$  at  $h \approx 10 \text{ nm}$ ; PSA-HS2) maximum energy barriers for the interactions of *P.*  
274 *ultimum* with T4 and PSA-HS2 phages, respectively (Table 2, Fig. 4). This indicates that both  
275 phages, if retained by the hyphae of *P. ultimum*, would be attracted directly to the primary minimum  
276  $\Phi_{\text{min1}}$ . However, no T4 phage) and a very weak secondary minimum ( $\Phi_{\text{min2}} = -2.7 \times 10^{-4} \text{ k}_B\text{T}$  at  $h \approx$   
277 12 nm) for PSA-HS2 phage was calculated and, hence, poor reversible retention of both phages by *P.*  
278 *ultimum* surfaces predicted by the XDLVO approach.<sup>63,64</sup> For interactions of the hyphal surface of *C.*  
279 *cinerea*, the XDLVO approach predicted the absence of  $\Phi_{\text{max1}}$  for both phages and more negative  
280 primary minima than for *P. ultimum* (Table 2, Fig. 4). No secondary minima were found, yet  
281 attractive  $G_{\text{XDLVO}}$  values, however, were calculated up to  $h \approx 100 \text{ nm}$  and  $h \approx 40 \text{ nm}$  above the *C.*  
282 *cinerea* hyphal surfaces for T4 and PSA-HS2 phages, respectively.

283

## 284 DISCUSSION

### 285 Effect of mycelia on phage transport and retention

286 We studied the interactions between phages and mycelia at the micrometer scale using a bespoke  
287 microfluidic platform. The so-called “Soil-on-a-Chip” microfluidic technology for organismal  
288 studies is an emerging field,<sup>65</sup> which allows for the precise control of the physico-chemical

289 microenvironment, high-resolution imaging and the simulation of environmental complexity on the  
290 microscale.<sup>66</sup> We assessed the interaction of phages with hyphae both in a quantitative manner and at  
291 the level of single hyphae. To our knowledge, this is the first study of its kind to analyze the role of  
292 hyphae on the transport and retention of nano-sized particles (phages). For this purpose, two lytic  
293 phages of different morphology and physical-chemical properties were applied, i.e., the T4 coli-  
294 phage and the marine phage PSA-HS2. The phages were injected into microfluidic channels  
295 containing growing mycelia of known structure and differing hydrophobicity and the time-averaged  
296 retention of the phages was calculated. Mycelia of the oomycete *P. ultimum* and of the hydrophobic  
297 agaricomycete *C. cinerea* were employed. Phage decay due to experimental conditions in the  
298 absence of mycelia was negligible and accounted for in our experiments. . Our data suggest that  
299 passage through microfluidic devices in the presence of moderately hydrophobic mycelia (*P.*  
300 *ultimum*) didn't lead to statistically verifiable phage retention (Table 2). The highly hydrophobic  
301 mycelia of *C. cinerea*, however, efficiently retained both phages (as reflected by increased  $R_P$  values)  
302 and significantly ( $p \leq 0.05$ ) reduced mass recovery (T4: > 93 %; PSA-HS2: and > 23 %) relative to  
303 mycelia free controls (Table 2). Differences in the phage recovery also demonstrate higher retention  
304 of the hydrophobic phage T4 than of the more hydrophilic PSA-HS2 phage. Most likely due to  
305 saturation of possible sorption sites, T4 however, showed no significant additional retention by *C.*  
306 *cinerea* in the observation period up to 22 h (Fig. 2D) while apparent saturation of the hyphal surface  
307 for PSA-HS2 phages was not yet reached (Fig. 2C). Our findings are consistent with previous  
308 studies showing that hydrophobic phages (and other viruses) are more efficiently retained than  
309 hydrophilic phages<sup>67,68,22</sup> They further reveal that sorption of viruses strongly depends on the surface  
310 properties of both the viruses and the sorbent; for instance, positively charged sorbents have been  
311 considered as ideal materials for the removal of viruses from aqueous systems.<sup>69,70</sup> Our results  
312 likewise emphasize for the first time the role of hydrophobic interactions for the interaction between  
313 phages and hyphal surfaces.<sup>67</sup>

314 As hyphal metabolites or extracellular products are known to foster coagulation<sup>71,39</sup> and hence may  
315 reduce colloidal stability and possible infectivity of phages, we further studied the impact of mycelial  
316 conditioned media on the infectivity of T4 and PSA-HS2 phage suspensions. With the exception of a  
317 slight (14 %) reduction of T4 phage counts after 22 h, no influence of mycelial conditioned media on  
318 total phage counts (i.e., phage infectivity) was observed (Fig. S1). Similar to the known effect of  
319 solid matrices,<sup>72,73</sup> it even may be speculated that fungal surfaces may protect viruses from  
320 inactivation.<sup>72,73</sup> The reasons for the reduction of T4 phages in the presence of *C. cinerea*  
321 conditioned medium after 22 h remain though unclear, yet are likely to be explained by the effect of  
322 extracellular mycelial products in the conditioned media (e.g., glycoprotein mucilages) that may  
323 influence colloidal stability rather than the infectivity of T4 phages. An additional effect on the  
324 reduced T4 phage stability may be caused by the CCMM medium, as mycelia-free controls also  
325 exhibited stability of  $93 \pm 4$  % (Fig. S2). Our data hence suggest the absence of mycelial effects on  
326 the infectivity and colloidal stability of the phages in the microfluidic devices. They underpin the  
327 relevance of phage deposition as the main driver for the reduced mass recoveries observed in the  
328 presence of the hydrophobic surfaces of *C. cinerea*.

329

### 330 **Phage-hyphal surface interaction energies**

331 Phages are charged colloidal particles<sup>69</sup> and believed to follow the principles of colloid chemistry  
332 despite of their morphological and structural variability.<sup>54</sup> Applying the XDLVO approach, we  
333 calculated the surface interaction energies as a function of the surface-to-surface distance,  $h$ , for a  
334 phage approaching a mycelial surface (eq. 3, Fig. 4). The XDLVO interaction energy is characterized  
335 by the primary minimum ( $\Phi_{\min 1}$ ), the secondary minimum ( $\Phi_{\min 2}$ ) and the maximum energy barrier  
336 ( $\Phi_{\max 1}$ ).<sup>57</sup> The XDLVO calculations predicted poor interactions of T4 and PSA-HS2 phages with  
337 hyphal surfaces of *P. ultimum* as evidenced by shallow  $\Phi_{\min 2}$  ( $-3 \times 10^{-4}$  k<sub>B</sub>T) for the PSA-HS2  
338 phage<sup>64</sup> and poorly negative  $G_{\text{XDLVO}}$  profiles ( $> \approx -8 \times 10^{-4}$  k<sub>B</sub>T) at distances  $h > 10$  nm above the

339 surfaces for the T4 phage (Fig 4). Only at close distances ( $h < \approx 10$  nm) to the hyphal surface, phages  
340 with a small kinetic energy<sup>57</sup> would be able to overcome the very low maximum energy barriers and  
341 get (irreversibly) attached in the primary minimum. These predictions are in good agreement with  
342 our experimental results showing less phage retention by *P. ultimum* than by *C. cinerea* hyphal  
343 surfaces (Figs. 2 & 3). For the latter, the  $G_{\text{XDLVO}}$  profiles of T4 and PSA-HS2 interactions exhibited  
344 clearly negative  $G_{\text{XDLVO}}$  values up to  $h \approx 40$  nm (PSA-HS2:  $-1.73 \text{ k}_B\text{T}$  at  $h = 10$  nm to  $-0.06 \text{ k}_B\text{T}$  at  $h$   
345  $= 40$  nm) and up to  $h \approx 145$  nm (T4:  $-3.62 \text{ k}_B\text{T}$  at  $h = 10$  nm to  $-0.06 \text{ k}_B\text{T}$  at  $h = 145$  nm) respectively  
346 and thus remain attractive up to longer separation distances than for hyphal surfaces of *P. ultimum*  
347 (Fig. 4). the XDLVO predictions reflect the experimentally observed differences of retention of T4  
348 and PSA-HS2 phages by mycelia of *C. cinerea* and *P. ultimum* respectively (Fig. 2 & 3) and supports  
349 the applicability of XDLVO approach to study the interactions of phages with surfaces.<sup>60</sup>

350

### 351 **Implications for phage transport**

352 The mobilization of colloids or bio-colloids such as bacteria and viruses in soil often is triggered by,  
353 snowmelts, or thunderstorms or high-intensity rain events that lead to high loads of the seepage  
354 water.<sup>74</sup> Rapid waterborne transport thereby may occur along macro-pores, cracks, or faults of the  
355 partly saturated soil, and hence in cavities where mycelia and their thread-like, adaptive and fractal  
356 networks<sup>75,76,35,36</sup> may be typically found.<sup>77</sup> Depending on the soil type, filamentous fungi may  
357 exhibit dry weight biomasses of up to 45 t per ha<sup>33</sup> and corresponding hyphal lengths of up to  $10^2 \text{ m}$   
358  $\text{g}^{-1}$  (arable soil) -  $10^4 \text{ m g}^{-1}$  (forest soil). Given a retention of phages to the mycelial surface of  $R_P =$   
359  $10^7 \text{ PFU mm}^{-2}$  and a presumed hyphal diameter of  $10^{-5} \text{ m}$ , such fungal biomass would translate to a  
360 calculated mycelial surface of  $\approx 0.0031 - 0.3140 \text{ m}^2$  or a hypothetical phage retention potential of  $3$   
361  $\times 10^{10}$  to  $3 \times 10^{12}$  phages per gram of soil. This would correspond to 30 to 3000 times the reported  
362 average number of virus like particles per gram of soil,<sup>78,79</sup> and, hence, be an important location for  
363 phage retention. Some hyphae are also known to become hydrophobic,<sup>50</sup> when exposed to air in

364 unsaturated soil conditions or during periods of soil drying. Hydrophobic mycelia may retain phages  
365 particularly well when exposed to conditions of soil water flow during major rain events. A recent 1-  
366 year time-series analysis of virus-like particle abundances in soils along a transect with different  
367 land-use practices, for instance, proposed rainfall-induced mobilization of viruses and correlations  
368 between rainfall and virus abundances in non-forest sites.<sup>79</sup> Furthermore, the physico-chemical  
369 effects of phage and hyphal surface properties on phage retention to mycelia can influence the  
370 structure of soil; for instance, some hyphae exert polysaccharides and glycoprotein mucilages<sup>39</sup> that  
371 enable the aggregation of soil mineral particles and organic matter.<sup>71</sup> These aggregates play a crucial  
372 role in the retention of viruses due to exclusion effects at the pore-scale.<sup>80</sup> At the micrometer scale,  
373 fungi take advantage of the three-dimensional space in the soil.<sup>48</sup> Their small hyphal diameter, which  
374 is approximately 1/60<sup>th</sup> the thickness of roots, allows fungi to access tight spaces.<sup>30</sup> This promotes the  
375 possible role that hyphae may play in the transport of colloidal particles, as bonding forces tend to be  
376 stronger at smaller size scales.<sup>39</sup> Consequently, understanding phage-mycelial interactions may help  
377 in planning different environmental and health related applications. For instance, tracer phages,  
378 which exhibit less retention in the presence of fungal mycelia, will be better tracer phages for tracer  
379 studies in terrestrial ecosystems. On the other hand, fungal mycelia with high phage retention  
380 potential can be used in the design of filter systems to reduce or hinder the transport of undesirable  
381 entities, e.g., pathogenic viruses, bacteria or anthropogenic nanoparticles. Accordingly,  
382 investigations concerning the influence of mycelia on the retention of phages could be extended to  
383 nanoparticles, which will be of interest for different applications. Further, the retention of phages by  
384 mycelia may increase the phage accessibility to bacteria, influence the multifarious bacterial-fungal  
385 interactions,<sup>81,34</sup> and/or promote phage-induced gene mobility in microbiomes of the mycosphere.  
386 Future work will need to include studies under more complex environmental conditions.

387

## 388 **ACKNOWLEDGMENTS**

389 This study is part of the Collaborative Research Centre AquaDiva (CRC 1076 AquaDiva) at the  
390 Friedrich Schiller University Jena and the Helmholtz Centre for Environmental Research - UFZ and  
391 was funded by the Deutsche Forschungsgemeinschaft (DFG). C.E.S. also acknowledges financial  
392 support by the Swiss National Science Foundation (Ambizione Grant No. PZ00P2\_168005). The  
393 authors wish to thank Laura Sánchez Fontanet, Jana Reichenbach, Birgit Würz and Luisa Ciabbarri for  
394 skilled technical help as well as Bijing Xiong (UFZ) for the photograph of the microfluidic device  
395 used in Fig. 1C and the TOC. The authors further thank Tom Berthold, Anja Worrich and René  
396 Kallies for helpful discussions and Prof. M. Künzler (ETH Zürich) for kindly providing *C. cinerea*  
397 strain AmutBmut pMA412.

398

#### 399 **SUPPLEMENTARY MATERIAL**

400 Supporting Information is available and contains three figures and two tables.

401

#### 402 **CONFLICT OF INTEREST**

403 The authors declare that the research was conducted in the absence of any commercial or financial  
404 relationships that could be construed as a potential conflict of interest.

405

406 **FIGURE LEGENDS**

407

408 **Figure 1.** (A) Photograph of the microfluidic platform used to monitor phage-mycelial interactions.  
409 A mycelial inoculum was placed next to the lateral opening of the microfluidic device (made from  
410 poly(dimethylsiloxane) (PDMS) silicone elastomer), allowing hyphae to penetrate and grow into the  
411 observation channel via a constriction channel, as illustrated in the two-dimensional overview of the  
412 microchannel geometry (B). Hyphal growth was observed in the observation channel, as indicated by  
413 the red dotted frame in (B), using bright field or fluorescence microscopy. (C) A bright-field  
414 micrograph of *P. ultimum* hyphae (24 h post inoculation). (D) A fluorescence micrograph of *C.*  
415 *cinerea* hyphae (48 h post inoculation). The direction of hyphal growth was toward the outlet.

416

417 **Figure 2.** PSA-HS2 and T4 phage concentrations in the influent (light grey bars) and the effluent of  
418 the microfluidic devices in the absence (black) and presence (grey) of hyphae after 4 and 22 h of  
419 continuous flow ( $5 \mu\text{L h}^{-1}$ ). Phages were enumerated by plaque forming units (PFU) depicted by total  
420 (primary y-axis on the left hand side of each panel). Data represent averages and standard deviations  
421 of triplicate experiments (except for duplicates for PSA-HS2 with *C. cinerea*). The asterisks on top  
422 of the columns refer to statistically significant differences (determined using two-tailed t-test)  
423 between the effluent concentration (in the presence of hyphae) and the corresponding controls (i.e.  
424 influent concentration and effluent concentration in the absence of hyphae):  $p \leq 0.05$  (\*),  $p \leq 0.01$   
425 (\*\*), and  $p \leq 0.001$  (\*\*\*)).

426

427 **Figure 3.** Total number of T4 or PSA-HS2 phages retained per  $\text{mm}^2$  of the mycelial surface after 4 h  
428 of phage percolation through the microfluidic devices containing either hyphae of *P. ultimum* or *C.*  
429 *cinerea*. Data represent averages and standard deviations of triplicate experiments (except for

430 duplicates for PSA-HS2 & *C. cinerea*). Asterisks indicate significant differences, if present, between  
431 different phage and mycelia pairs:  $p \leq 0.01$  (\*\*) and  $p \leq 0.001$  (\*\*\*).

432

433 **Figure 4.** XDLVO interaction energy profiles between phages and mycelia. The interaction energy  
434 profiles show the overall interaction energy ( $G_{XDLVO}$ ; black solid line), the acid-base interaction  
435 energy ( $G_{AB}$ ; orange long-dashed line), the electrostatic repulsion ( $G_{EDL}$ ; blue short-dashed line),  
436 and the Lifshitz-van der Waals energy ( $G_{LW}$ ; red dotted-dashed line) as a function of distance  
437 particle  $h$  (nm) between the phage and the mycelia surface.

438 **Table 1.** Overview of the names, classifications, size and physico-chemical surface properties of the  
 439 phages and hyphal organisms used in this study.  
 440

441

Name (Name of family or class)	Phage host name	Zeta potential $\zeta$	Water contact angle $\Theta_w$	Size (head/tail)	Surface area
		(mV)	(degree)	( $\mu\text{m}$ )	( $\text{mm}^2$ )
PSA-HS2 ( <i>Siphoviridae</i> )	<i>Pseudoalteromonas</i> H13-15	$-10 \pm 1$	$40 \pm 5^{\text{a}}$	$0.21^{\text{a}}$ ( $0.06/0.15^{\text{a}}$ )	--
T4 ( <i>Myoviridae</i> )	<i>E. coli</i> (Migula 1895)	$-10 \pm 2$	$95 \pm 5^{\text{a}}$	$0.203^{\text{a}}$ ( $0.09/0.113^{\text{a}}$ )	--
<i>Pythium ultimum</i> (Oomycete)	--	$-11 \pm 3$	$62 \pm 6$	$10 \pm 3^{\text{b}}$	$1.2 \pm 0.1^{\text{c}}$
<i>Copriopsis cinerea</i> strain AmutBmut pMA412 (Agaricomycete)	--	$-13 \pm 4$	$131 \pm 2$	$7 \pm 1^{\text{b}}$	$0.9 \pm 0.4^{\text{c}}$

442

443 <sup>a)</sup> Data taken from Ghanem et al.<sup>22</sup> <sup>b)</sup> Average and standard deviations ( $n \geq 20$ ) of hyphal diameters, <sup>c)</sup> Average and standard deviations of  
 444 the surface area of mycelia ( $n > 5$ ) after 24 h (*P. ultimum*) and 48 h (*C. cinerea*) of inoculation.

445

446 **Table 2.** Calculated retention (RP) of phages to mycelial surfaces (0 - 4 h) and mass recoveries (*M*) of transport experiments in microfluidic  
 447 devices, as well as the stability and viability of phage suspensions in the presence of *P. ultimum* and *C. cinerea* conditioned media. The values of  
 448 the maximum energy barrier ( $\Phi_{\max 1}$ ), the primary minimum ( $\Phi_{\min 1}$ ), and the secondary minimum ( $\Phi_{\min 2}$ ) of phage-mycelia interaction energies  
 449 were derived based on the XDLVO approach using a sphere-plate model.

450

Phage name	Name of hyphal organisms	Retention of phages to mycelial surface (R <sub>p</sub> ) after 0 - 4 h <sup>a, b</sup>	Phage mass recovery with mycelia after 0 - 4 h (4 - 22 h) <sup>b</sup>	Phage mass recovery without mycelia after 0 - 4 h (4 - 22 h) <sup>b</sup>	Phage stability after 4 h (after 22 h) <sup>c</sup>	Calculated maximum energy barrier <sup>d</sup>	Calculated energy at primary minimum <sup>d</sup>	Calculated energy at secondary minimum <sup>d</sup>
			<i>M</i>	<i>M</i>		$\Phi_{\max 1}$	$\Phi_{\min 1}$	$\Phi_{\min 2}$
		(PFU mm <sup>-2</sup> × 10 <sup>6</sup> )	(%)	(%)	(%)	(k <sub>B</sub> T × 10 <sup>-3</sup> )	(k <sub>B</sub> T × 10 <sup>4</sup> )	(k <sub>B</sub> T × 10 <sup>-3</sup> )
<b>PSA-HS2</b>	<i>Pythium ultimum</i>	4.26 ± 0.6	92 ± 3 (108 ± 12)	98 ± 5 (94 ± 0)	97 ± 23 (98 ± 16)	4.7	-1.1	-0.3
	<i>Coprinopsis cinerea</i>	13.6 ± 1.3	77 ± 2 (75 ± 6)	99 ± 0.2 (97 ± 0)	102 ± 11 (99 ± 16)	na <sup>e</sup>	-1.9	na <sup>d</sup>
<b>T4</b>	<i>Pythium ultimum</i>	2.3 ± 0.8	98 ± 4 (107 ± 15)	99 ± 1 (109 ± 7)	108 ± 6 (94 ± 3)	na <sup>e</sup>	-14	na <sup>e</sup>
	<i>Coprinopsis cinerea</i>	36.7 ± 0.61	7 ± 1 (86 ± 11)	98 ± 5 (92 ± 0.5)	106 ± 5 (86 ± 6)	na <sup>e</sup>	-29	na <sup>e</sup>

451

452 <sup>a)</sup> Values are corrected for losses in the absence of mycelia (cf. eq. 2). <sup>b)</sup> Influent concentrations of phages (PFU mL<sup>-1</sup>): PSA-HS2 and *P. ultimum*: 1.7 × 10<sup>9</sup>, PSA-HS2 and *C. cinerea*: 3.4 × 10<sup>9</sup>, T4 and *P. ultimum*: 3.3  
 453 × 10<sup>9</sup>; T4 and *C. cinerea*: 2.6 × 10<sup>9</sup> PFU mL<sup>-1</sup>. <sup>c)</sup> Phage stability in the presence of cell-free conditioned media. <sup>d)</sup> As predicted by XDLVO interaction energy profiles (cf. eq. 3, Fig. 4). <sup>e)</sup> No value could be calculated.

454

455

456 **REFERENCES**

- 457 (1) Paul, J. H.; Rose, J. B.; Brown, J.; Shinn, E. A.; Miller, S.; Farrah, S. R. Viral Tracer Studies  
 458 Indicate Contamination of Marine Waters by Sewage Disposal Practices in Key Largo, Florida. *Appl.*  
 459 *Environ. Microbiol.* **1995**, *61* (6), 2230–2234.
- 460 (2) Williamson, K. E.; Harris, J. V.; Green, J. C.; Rahman, F.; Chambers, R. M. Stormwater  
 461 Runoff Drives Viral Community Composition Changes in Inland Freshwaters. *Front. Microbiol.*  
 462 **2014**, *5*, 105. <https://doi.org/10.3389/fmicb.2014.00105>.
- 463 (3) Collins, K. E.; Cronin, A. A.; Rueedi, J.; Pedley, S.; Joyce, E.; Humble, P. J.; Tellam, J. H.  
 464 Fate and Transport of Bacteriophage in UK Aquifers as Surrogates for Pathogenic Viruses. *Eng.*  
 465 *Geol.* **2006**, *85* (1–2), 33–38. <https://doi.org/10.1016/j.enggeo.2005.09.025>.
- 466 (4) McKay, L. D.; Cherry, J. A.; Bales, R. C.; Yahya, M. T.; Gerba, C. P. A Field Example of  
 467 Bacteriophage as Tracers of Fracture Flow. *Environ. Sci. Technol.* **1993**, *27* (6), 1075–1079.
- 468 (5) Flynn, R. M.; Mallèn, G.; Engel, M.; Ahmed, A.; Rossi, P. Characterizing Aquifer  
 469 Heterogeneity Using Bacterial and Bacteriophage Tracers. *J. Environ. Qual.* **2015**, *44* (5), 1448.  
 470 <https://doi.org/10.2134/jeq2015.02.0117>.
- 471 (6) Harvey, R. W.; Harms, H.; Landkamer, L. Transport of Microorganisms in the Terrestrial  
 472 Subsurface: In Situ and Laboratory Methods. *Man. Environ. Microbiol.* **2002**, *2*, 753–776.
- 473 (7) Rossi, P. Advances in biological tracer techniques for hydrology and hydrogeology using  
 474 bacteriophages, Université de Neuchâtel, 1994.
- 475 (8) Flynn, R.; Hunkeler, D.; Guerin, C.; Burn, C.; Rossi, P.; Aragno, M. Geochemical Influences  
 476 on H40/1 Bacteriophage Inactivation in Glaciofluvial Sands. *Environ. Geol.* **2004**, *45* (4), 504–517.
- 477 (9) Goldscheider, N.; Haller, L.; Poté, J.; Wildi, W.; Zopfi, J. Characterizing Water Circulation  
 478 and Contaminant Transport in Lake Geneva Using Bacteriophage Tracer Experiments and  
 479 Limnological Methods. *Environ. Sci. Technol.* **2007**, *41* (15), 5252–5258.  
 480 <https://doi.org/10.1021/es070369p>.
- 481 (10) Flynn, R. M.; Sinreich, M. Characterisation of Virus Transport and Attenuation in Epikarst  
 482 Using Short Pulse and Prolonged Injection Multi-Tracer Testing. *Water Res.* **2010**, *44* (4), 1138–  
 483 1149. <https://doi.org/10.1016/j.watres.2009.11.032>.
- 484 (11) Zhao, B.; Zhang, H.; Zhang, J.; Jin, Y. Virus Adsorption and Inactivation in Soil as  
 485 Influenced by Autochthonous Microorganisms and Water Content. *Soil Biol. Biochem.* **2008**, *40* (3),  
 486 649–659. <https://doi.org/10.1016/j.soilbio.2007.09.020>.
- 487 (12) Moore, R. S.; Taylor, D. H.; Sturman, L. S.; Reddy, M. M.; Fuhs, G. W. Poliovirus  
 488 Adsorption by 34 Minerals and Soils. *Appl. Environ. Microbiol.* **1981**, *42* (6), 963–975.
- 489 (13) Van Cuyk, S.; Siegrist, R. L. Virus Removal within a Soil Infiltration Zone as Affected by  
 490 Effluent Composition, Application Rate, and Soil Type. *Water Res.* **2007**, *41* (3), 699–709.  
 491 <https://doi.org/10.1016/j.watres.2006.07.021>.

- 492 (14) Kinoshita, T.; Bales, R. C.; Maguire, K. M.; Gerba, C. P. Effect of PH on Bacteriophage  
493 Transport through Sandy Soils. *J. Contam. Hydrol.* **1993**, *14* (1), 55–70.  
494 [https://doi.org/10.1016/0169-7722\(93\)90041-P](https://doi.org/10.1016/0169-7722(93)90041-P).
- 495 (15) Carlson, G. F.; Woodard, F. E.; Wentworth, D. F.; Sproul, O. J. Virus Inactivation on Clay  
496 Particles in Natural Waters. *J. Water Pollut. Control Fed.* **1968**, *40* (2), R89–R106.
- 497 (16) Taylor, D. H.; Moore, R. S.; Sturman, L. S. Influence of PH and Electrolyte Composition on  
498 Adsorption of Poliovirus by Soils and Minerals. *Appl. Environ. Microbiol.* **1981**, *42* (6), 976–984.
- 499 (17) Lance, J. C.; Gerba, C. P. Effect of Ionic Composition of Suspending Solution on Virus  
500 Adsorption by a Soil Column. *Appl. Environ. Microbiol.* **1984**, *47* (3), 484–488.
- 501 (18) Anders, R.; Chrysikopoulos, C. V. Transport of Viruses Through Saturated and Unsaturated  
502 Columns Packed with Sand. *Transp. Porous Media* **2009**, *76* (1), 121–138.  
503 <https://doi.org/10.1007/s11242-008-9239-3>.
- 504 (19) Trouwborst, T.; Kuyper, S.; De Jong, J. C.; Plantinga, A. D. Inactivation of Some Bacterial  
505 and Animal Viruses by Exposure to Liquid–Air Interfaces. *J. Gen. Virol.* **1974**, *24* (1), 155–165.
- 506 (20) Dika, C.; Duval, J. F. L.; Francius, G.; Perrin, A.; Gantzer, C. Isoelectric Point Is an  
507 Inadequate Descriptor of MS2, Phi X 174 and PRD1 Phages Adhesion on Abiotic Surfaces. *J.*  
508 *Colloid Interface Sci.* **2015**, *446*, 327–334. <https://doi.org/10.1016/j.jcis.2014.08.055>.
- 509 (21) Dowd, S. E.; Pillai, S. D.; Wang, S.; Corapcioglu, M. Y. Delineating the Specific Influence of  
510 Virus Isoelectric Point and Size on Virus Adsorption and Transport through Sandy Soils. *Appl.*  
511 *Environ. Microbiol.* **1998**, *64* (2), 405–410.
- 512 (22) Ghanem, N.; Kiesel, B.; Kallies, R.; Harms, H.; Chatzinotas, A.; Wick, L. Y. Marine Phages  
513 As Tracers: Effects of Size, Morphology, and Physico–Chemical Surface Properties on Transport in  
514 a Porous Medium. *Environ. Sci. Technol.* **2016**, *50* (23), 12816–12824.  
515 <https://doi.org/10.1021/acs.est.6b04236>.
- 516 (23) Küsel, K.; Totsche, K. U.; Trumbore, S. E.; Lehmann, R.; Steinhäuser, C.; Herrmann, M.  
517 How Deep Can Surface Signals Be Traced in the Critical Zone? Merging Biodiversity with  
518 Biogeochemistry Research in a Central German Muschelkalk Landscape. *Front. Earth Sci.* **2016**, *4*,  
519 32. <https://doi.org/10.3389/feart.2016.00032>.
- 520 (24) John, D. E.; Rose, J. B. Review of Factors Affecting Microbial Survival in Groundwater.  
521 *Environ. Sci. Technol.* **2005**, *39* (19), 7345–7356. <https://doi.org/10.1021/es047995w>.
- 522 (25) Hurst, C. J. Influence of Aerobic Microorganisms upon Virus Survival in Soil. *Can. J.*  
523 *Microbiol.* **1988**, *34* (5), 696–699.
- 524 (26) Sobsey, M. D.; Dean, C. H.; Knuckles, M. E.; Wagner, R. A. Interactions and Survival of  
525 Enteric Viruses in Soil Materials. *Appl. Environ. Microbiol.* **1980**, *40* (1), 92–101.
- 526 (27) Campbell, R. N. Fungal Transmission of Plant Viruses. *Annu. Rev. Phytopathol.* **1996**, *34* (1),  
527 87–108.
- 528 (28) Alfaro-Fernández, A.; Del Carmen Córdoba-Sellés, M.; Herrera-Vásquez, J. Á.; Cebrián, M.  
529 del C.; Jordá, C. Transmission of Pepino Mosaic Virus by the Fungal Vector *Olpidium Virulentus*. *J.*  
530 *Phytopathol.* **2010**, *158* (4), 217–226. <https://doi.org/10.1111/j.1439-0434.2009.01605.x>.

- 531 (29) Varanda, C. M. R.; Silva, M. S. M. R.; Félix, M. do R. F.; Clara, M. I. E. Evidence of Olive  
532 Mild Mosaic Virus Transmission by *Olpidium Brassicae*. *Eur. J. Plant Pathol.* **2011**, *130* (2), 165–  
533 172. <https://doi.org/10.1007/s10658-011-9742-1>.
- 534 (30) Pennisi, E. The Secret Life of Fungi. *Science* **2004**, *304* (5677), 1620.
- 535 (31) Kendrick, B. *The Fifth Kingdom*; Focus Pub., 2000.
- 536 (32) Kohlmeier, S.; Smits, T. H. M.; Ford, R. M.; Keel, C.; Harms, H.; Wick, L. Y. Taking the  
537 Fungal Highway: Mobilization of Pollutant-Degrading Bacteria by Fungi. *Environ. Sci. Technol.*  
538 **2005**, *39* (12), 4640–4646. <https://doi.org/10.1021/es047979z>.
- 539 (33) Harms, H.; Schlosser, D.; Wick, L. Y. Untapped Potential: Exploiting Fungi in  
540 Bioremediation of Hazardous Chemicals. *Nat. Rev. Microbiol.* **2011**, *9* (3), 177–192.  
541 <https://doi.org/10.1038/nrmicro2519>.
- 542 (34) Deveau, A.; Bonito, G.; Uehling, J.; Paoletti, M.; Becker, M.; Bindschedler, S.; Hacquard, S.;  
543 Hervé, V.; Labbé, J.; Lastovetsky, O. A.; Mieszkin, S.; Millet, L.J.; Vajna, B.; Junier, P.; Bonfante,  
544 P.; Krom, B.P.; Olsson, S.; van Elsas, J.D.; Wick, L.Y.. Bacterial-Fungal Interactions: Ecology,  
545 Mechanisms and Challenges. *FEMS Microbiol. Rev.* **2018**, *42* (3), 335–352.  
546 <https://doi.org/10.1093/femsre/fuy008>.
- 547 (35) Berthold, T.; Centler, F.; Hübschmann, T.; Remer, R.; Thullner, M.; Harms, H.; Wick, L. Y.  
548 Mycelia as a Focal Point for Horizontal Gene Transfer among Soil Bacteria. *Sci. Rep.* **2016**, *6*.  
549 <https://doi.org/10.1038/srep36390>.
- 550 (36) Zhang, M.; Silva, P. e; C, M. de; De Mares Maryam, C.; Elsas, V.; Dirk, J. The Mycosphere  
551 Constitutes an Arena for Horizontal Gene Transfer with Strong Evolutionary Implications for  
552 Bacterial-Fungal Interactions. *FEMS Microbiol. Ecol.* **2014**, *89* (3), 516–526.  
553 <https://doi.org/10.1111/1574-6941.12350>.
- 554 (37) Wösten, H. A. B.; van Wetter, M.-A.; Lugones, L. G.; van der Mei, H. C.; Busscher, H. J.;  
555 Wessels, J. G. H. How a Fungus Escapes the Water to Grow into the Air. *Curr. Biol.* **1999**, *9* (2), 85–  
556 88. [https://doi.org/10.1016/S0960-9822\(99\)80019-0](https://doi.org/10.1016/S0960-9822(99)80019-0).
- 557 (38) Smits, M. M.; Herrmann, A. M.; Duane, M.; Duckworth, O. W.; Bonneville, S.; Benning, L.  
558 G.; Lundström, U. The Fungal–mineral Interface: Challenges and Considerations of Micro-  
559 Analytical Developments. *Fungal Biol. Rev.* **2009**, *23* (4), 122–131.  
560 <https://doi.org/10.1016/j.fbr.2009.11.001>.
- 561 (39) Ritz, K.; Young, I. M. Interactions between Soil Structure and Fungi. *Mycologist* **2004**, *18*  
562 (2), 52–59.
- 563 (40) Deng, L.; Gregory, A.; Yilmaz, S.; Poulos, B. T.; Hugenholtz, P.; Sullivan, M. B. Contrasting  
564 Life Strategies of Viruses That Infect Photo- and Heterotrophic Bacteria, as Revealed by Viral  
565 Tagging. *mBio* **2012**, *3* (6), e00373-12-e00373-12. <https://doi.org/10.1128/mBio.00373-12>.
- 566 (41) Clokie, M. R.; Millard, A. D.; Letarov, A. V.; Heaphy, S. Phages in Nature. *Bacteriophage*  
567 **2011**, *1* (1), 31–45.
- 568 (42) Hijnen, W. A. M.; Brouwer-Hanzens, A. J.; Charles, K. J.; Medema, G. J. Transport of MS2  
569 Phage, *Escherichia Coli*, *Clostridium Perfringens*, *Cryptosporidium Parvum*, and *Giardia*  
570 *Intestinalis* in a Gravel and a Sandy Soil. *Environ. Sci. Technol.* **2005**, *39* (20), 7860–7868.  
571 <https://doi.org/10.1021/es050427b>.

- 572 (43) Mohn, G.; Ellenberger, J.; McGregor, D. Development of Mutagenicity Test Using  
573 Escherichia Coli K-12 as Indicator Organism. *Mutat. Res.* **1974**, *25* (2), 187–196.
- 574 (44) Duhaimé, M. B.; Solonenko, N.; Roux, S.; Verberkmoes, N. C.; Wichels, A.; Sullivan, M. B.  
575 Comparative Omics and Trait Analyses of Marine Pseudoalteromonas Phages Advance the Phage  
576 OTU Concept. *Front. Microbiol.* **2017**, *8*. <https://doi.org/10.3389/fmicb.2017.01241>.
- 577 (45) Oppenheimer, C.; Zobell, C. The Growth and Viability of 63 Species of Marine Bacteria as  
578 Influenced. *J. Mar. Res.* **1952**, *11* (1), 10–18.
- 579 (46) Sezonov, G.; Joseleau-Petit, D.; D’Ari, R. Escherichia Coli Physiology in Luria-Bertani  
580 Broth. *J. Bacteriol.* **2007**, *189* (23), 8746–8749. <https://doi.org/10.1128/JB.01368-07>.
- 581 (47) Stanley, C. E.; Stöckli, M.; Swaay, D. van; Sabotič, J.; Kallio, P. T.; Künzler, M.; deMello,  
582 A. J.; Aebi, M. Probing Bacterial–fungal Interactions at the Single Cell Level. *Integr. Biol.* **2014**, *6*  
583 (10), 935–945. <https://doi.org/10.1039/C4IB00154K>.
- 584 (48) Furuno, S.; Pätzolt, K.; Rabe, C.; Neu, T. R.; Harms, H.; Wick, L. Y. Fungal Mycelia Allow  
585 Chemotactic Dispersal of Polycyclic Aromatic Hydrocarbon-Degrading Bacteria in Water-  
586 Unsaturated Systems. *Environ. Microbiol.* **2010**, *12* (6), 1391–1398. <https://doi.org/10.1111/j.1462-2920.2009.02022.x>.
- 588 (49) Thompson, S. S.; Flury, M.; Yates, M. V.; Jury, W. A. Role of the Air-Water-Solid Interface  
589 in Bacteriophage Sorption Experiments. *Appl. Environ. Microbiol.* **1998**, *64* (1), 304–309.
- 590 (50) Smits, T. H. M.; Wick, L. Y.; Harms, H.; Keel, C. Characterization of the Surface  
591 Hydrophobicity of Filamentous Fungi. *Environ. Microbiol.* **2003**, *5* (2), 85–91.
- 592 (51) Stanley, C.; Shrivastava, J.; Brugman, R.; Heinzelmann, E.; Frajs, V.; Bühler, A.; van Swaay,  
593 D.; Grossmann, G. Fabrication and Use of the Dual-Flow-RootChip for the Imaging of Arabidopsis  
594 Roots in Asymmetric Microenvironments. *BIO-Protoc.* **2018**, *8* (18).  
595 <https://doi.org/10.21769/BioProtoc.3010>.
- 596 (52) Schneider, C. A.; Rasband, W. S.; Eliceiri, K. W. NIH Image to ImageJ: 25 Years of Image  
597 Analysis. *Nat. Methods* **2012**, *9* (7), 671.
- 598 (53) Jensen, E. C. Quantitative Analysis of Histological Staining and Fluorescence Using ImageJ.  
599 *Anat. Rec.* **2013**, *296* (3), 378–381. <https://doi.org/10.1002/ar.22641>.
- 600 (54) Syngouna, V. I.; Chrysikopoulos, C. V. Transport of Biocolloids in Water Saturated Columns  
601 Packed with Sand: Effect of Grain Size and Pore Water Velocity. *J. Contam. Hydrol.* **2011**, *126* (3–  
602 4), 301–314. <https://doi.org/10.1016/j.jconhyd.2011.09.007>.
- 603 (55) Boks, N. P.; Norde, W.; van der Mei, H. C.; Busscher, H. J. Forces Involved in Bacterial  
604 Adhesion to Hydrophilic and Hydrophobic Surfaces. *Microbiology* **2008**, *154* (10), 3122–3133.  
605 <https://doi.org/10.1099/mic.0.2008/018622-0>.
- 606 (56) Bergendahl, J.; Grasso, D. Prediction of Colloid Detachment in a Model Porous Media:  
607 Thermodynamics. *AIChE J.* **1999**, *45* (3), 475–484. <https://doi.org/10.1002/aic.690450305>.
- 608 (57) Chrysikopoulos, C. V.; Syngouna, V. I. Attachment of Bacteriophages MS2 and \_X174 onto  
609 Kaolinite and Montmorillonite: Extended-DLVO Interactions. *Colloids Surf. B Biointerfaces* **2012**,  
610 *92*, 74–83. <https://doi.org/10.1016/j.colsurfb.2011.11.028>.

- 611 (58) van Oss, C. J.; Docoslis, A.; Wu, W.; Giese, R. F. Influence of Macroscopic and Microscopic  
612 Interactions on Kinetic Rate Constants: I. Role of the Extended DLVO Theory in Determining the  
613 Kinetic Adsorption Constant of Proteins in Aqueous Media, Using von Smoluchowski's Approach.  
614 *Colloids Surf. B Biointerfaces* **1999**, *14* (1–4), 99–104. [https://doi.org/10.1016/S0927-7765\(99\)00028-4](https://doi.org/10.1016/S0927-7765(99)00028-4).  
615
- 616 (59) Mulligan, A. E.; Charette, M. A. Groundwater Flow to the Coastal Ocean. In *Encyclopedia of*  
617 *Ocean Sciences (Second Edition)*; Steele, J. H., Ed.; Academic Press: Oxford, 2009; pp 88–97.  
618 <https://doi.org/10.1016/B978-012374473-9.00645-7>.
- 619 (60) Hermansson, M. The DLVO Theory in Microbial Adhesion. *Colloids Surf. B Biointerfaces*  
620 **1999**, *14* (1), 105–119.
- 621 (61) van Loosdrecht, M. C.; Lyklema, J.; Norde, W.; Zehnder, A. J. Bacterial Adhesion: A  
622 Physicochemical Approach. *Microb. Ecol.* **1989**, *17* (1), 1–15.
- 623 (62) Jucker, B. A. Polymer Interactions and Bacterial Adhesion. PhD Thesis, ETH Zurich, 1998.
- 624 (63) Hahn, M. W.; O'Melia, C. R. Deposition and Reentrainment of Brownian Particles in Porous  
625 Media under Unfavorable Chemical Conditions: Some Concepts and Applications. *Environ. Sci.*  
626 *Technol.* **2004**, *38* (1), 210–220. <https://doi.org/10.1021/es030416n>.
- 627 (64) Shen, C.; Li, B.; Huang, Y.; Jin, Y. Kinetics of Coupled Primary- and Secondary-Minimum  
628 Deposition of Colloids under Unfavorable Chemical Conditions. *Environ. Sci. Technol.* **2007**, *41*  
629 (20), 6976–6982. <https://doi.org/10.1021/es070210c>.
- 630 (65) Stanley, C. E.; Grossmann, G.; Solvas, X. C. i; deMello, A. J. Soil-on-a-Chip: Microfluidic  
631 Platforms for Environmental Organismal Studies. *Lab. Chip* **2016**, *16* (2), 228–241.  
632 <https://doi.org/10.1039/C5LC01285F>.
- 633 (66) Stanley, C. E.; Heijden, M. G. A. van der. Microbiome-on-a-Chip: New Frontiers in Plant–  
634 Microbiota Research. *Trends Microbiol.* **2017**, *25* (8), 610–613.  
635 <https://doi.org/10.1016/j.tim.2017.05.001>.
- 636 (67) Attinti, R.; Wei, J.; Kniel, K.; Sims, J. T.; Jin, Y. Virus' (MS2, ΦX174, and Aichi)  
637 Attachment on Sand Measured by Atomic Force Microscopy and Their Transport through Sand  
638 Columns. *Environ. Sci. Technol.* **2010**, *44* (7), 2426–2432. <https://doi.org/10.1021/es903221p>.
- 639 (68) Dika, C.; Ly-Chatain, M. H.; Francius, G.; Duval, J. F. L.; Gantzer, C. Non-DLVO Adhesion  
640 of F-Specific RNA Bacteriophages to Abiotic Surfaces: Importance of Surface Roughness,  
641 Hydrophobic and Electrostatic Interactions. *Colloids Surf. Physicochem. Eng. Asp.* **2013**, *435*, 178–  
642 187. <https://doi.org/10.1016/j.colsurfa.2013.02.045>.
- 643 (69) You, Y.; Vance, G. F.; Sparks, D. L.; Zhuang, J.; Jin, Y. Sorption of MS2 Bacteriophage to  
644 Layered Double Hydroxides. *J. Environ. Qual.* **2003**, *32* (6), 2046–2053.
- 645 (70) Schijven, J. F.; Hassanizadeh, S. M. Removal of Viruses by Soil Passage: Overview of  
646 Modeling, Processes, and Parameters. *Crit. Rev. Environ. Sci. Technol.* **2000**, *30* (1), 49–127.  
647 <https://doi.org/10.1080/10643380091184174>.
- 648 (71) Bardgett, R. *The Biology of Soil: A Community and Ecosystem Approach*; Biology of  
649 Habitats Series; Oxford University Press: Oxford, New York, 2005.

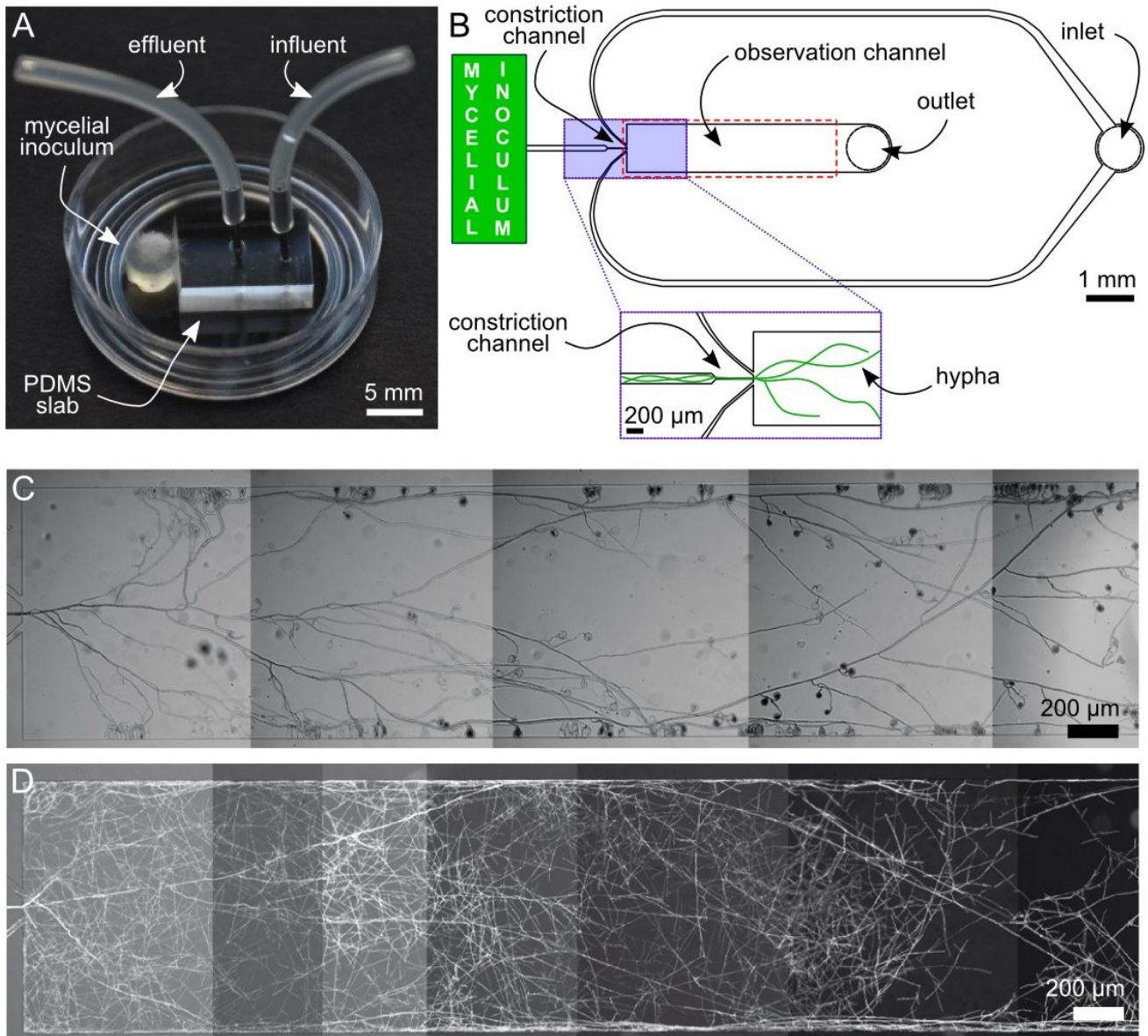
- 650 (72) Chrysikopoulos, C. V.; Aravantinou, A. F. Virus Inactivation in the Presence of Quartz Sand  
651 under Static and Dynamic Batch Conditions at Different Temperatures. *J. Hazard. Mater.* **2012**,  
652 233–234, 148–157. <https://doi.org/10.1016/j.jhazmat.2012.07.002>.
- 653 (73) Pecson, B. M.; Decrey, L.; Kohn, T. Photoinactivation of Virus on Iron-Oxide Coated Sand:  
654 Enhancing Inactivation in Sunlit Waters. *Water Res.* **2012**, 46 (6), 1763–1770.  
655 <https://doi.org/10.1016/j.watres.2011.12.059>.
- 656 (74) Totsche, K. U.; Jann, S.; Kögel-Knabner, I. Single Event–Driven Export of Polycyclic  
657 Aromatic Hydrocarbons and Suspended Matter from Coal Tar–Contaminated Soil. *Vadose Zone J.*  
658 **2007**, 6 (2), 233–243. <https://doi.org/10.2136/vzj2006.0083>.
- 659 (75) Worrich, A.; Wick, L. Y.; Banitz, T. Chapter Three - Ecology of Contaminant  
660 Biotransformation in the Mycosphere: Role of Transport Processes. In *Advances in Applied*  
661 *Microbiology*; Gadd, G. M., Sariaslani, S., Eds.; Academic Press, 2018; Vol. 104, pp 93–133.  
662 <https://doi.org/10.1016/bs.aambs.2018.05.005>.
- 663 (76) Fester, T.; Giebler, J.; Wick, L. Y.; Schlosser, D.; Kästner, M. Plant–microbe Interactions as  
664 Drivers of Ecosystem Functions Relevant for the Biodegradation of Organic Contaminants. *Curr.*  
665 *Opin. Biotechnol.* **2014**, 27, 168–175. <https://doi.org/10.1016/j.copbio.2014.01.017>.
- 666 (77) Otten, W.; Hall, D.; Harris, K.; Ritz, K.; Young, I. M.; Gilligan, C. A. Soil Physics, Fungal  
667 Epidemiology and the Spread of Rhizoctonia Solani. *New Phytol.* **2001**, 151 (2), 459–468.  
668 <https://doi.org/10.1046/j.0028-646x.2001.00190.x>.
- 669 (78) Williamson, K. E.; Radosevich, M.; Wommack, K. E. Abundance and Diversity of Viruses in  
670 Six Delaware Soils. *Appl. Environ. Microbiol.* **2005**, 71 (6), 3119–3125.  
671 <https://doi.org/10.1128/AEM.71.6.3119-3125.2005>.
- 672 (79) Narr, A.; Nawaz, A.; Wick, L. Y.; Harms, H.; Chatzinotas, A. Soil Viral Communities Vary  
673 Temporally and along a Land Use Transect as Revealed by Virus-Like Particle Counting and a  
674 Modified Community Fingerprinting Approach (FRAPD). *Front. Microbiol.* **2017**, 8.  
675 <https://doi.org/10.3389/fmicb.2017.01975>.
- 676 (80) Sirivithayapakorn, S.; Keller, A. Transport of Colloids in Saturated Porous Media: A Pore-  
677 Scale Observation of the Size Exclusion Effect and Colloid Acceleration. *Water Resour. Res.* **2003**,  
678 39 (4), n/a-n/a. <https://doi.org/10.1029/2002WR001583>.
- 679 (81) Worrich, A.; Wick, L. Y.; Banitz, T. Ecology of Contaminant Biotransformation in the  
680 Mycosphere: Role of Transport Processes. *Adv. Appl. Microbiol.* **2018**, 104, 93–133.  
681 <https://doi.org/10.1016/bs.aambs.2018.05.005>.
- 682 (82) Pratama, A. A. and van Elsas J. D.; Gene mobility in microbiomes of the mycosphere and  
683 mycorrhizosphere –role of plasmids and bacteriophages. *FEMS Microbiol. Ecol.* **2019**, 95, Issue 5,  
684 fiz053, <https://doi.org/10.1093/femsec/fiz053>.

685

686

687 **FIGURES**

688



689

690

691 **Figure 1**

692

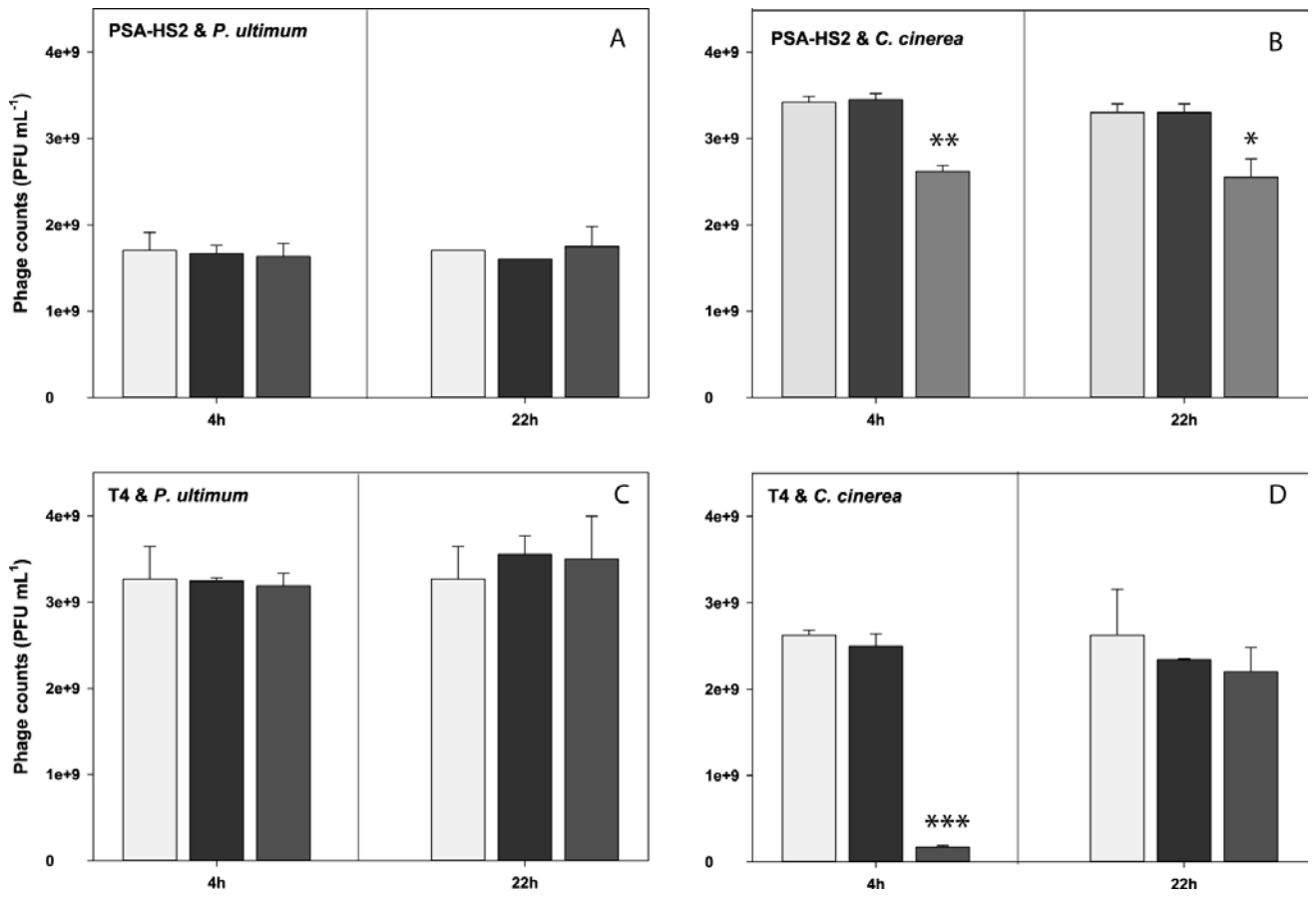
693

694

695

696

697



699

700

Figure 2

701

702

703

704

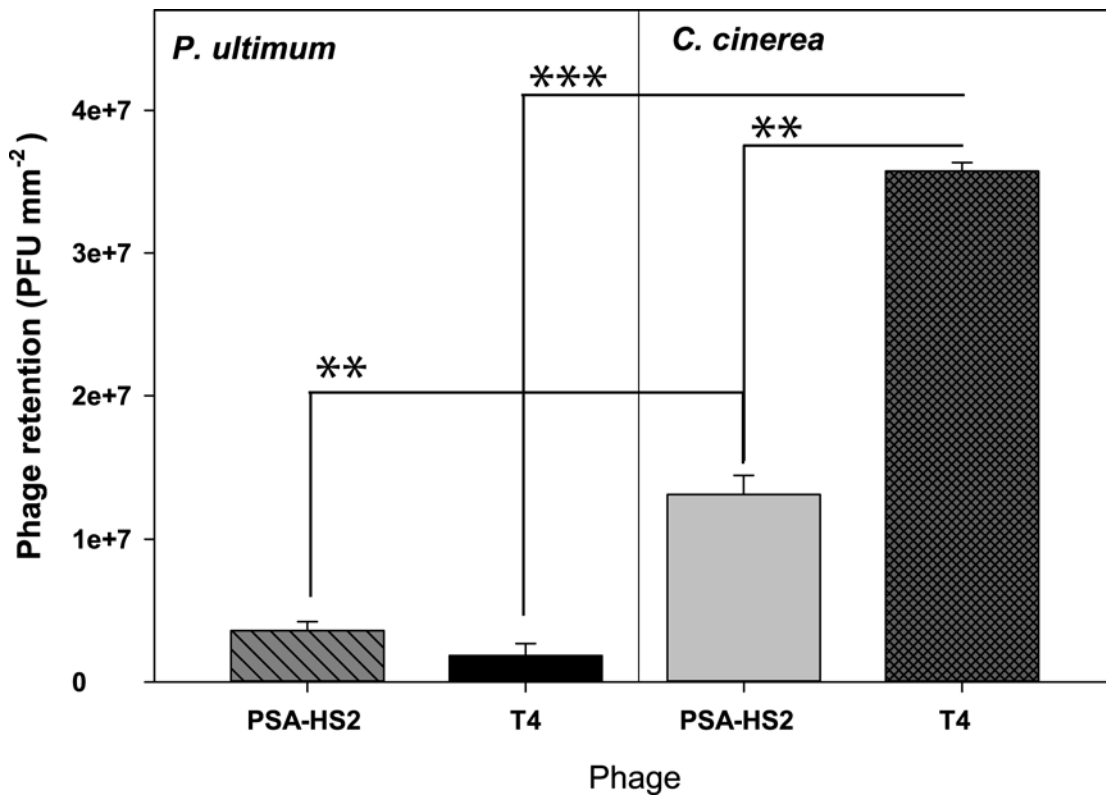
705

706

707

708

709



710

711 **Figure 3**

712

713

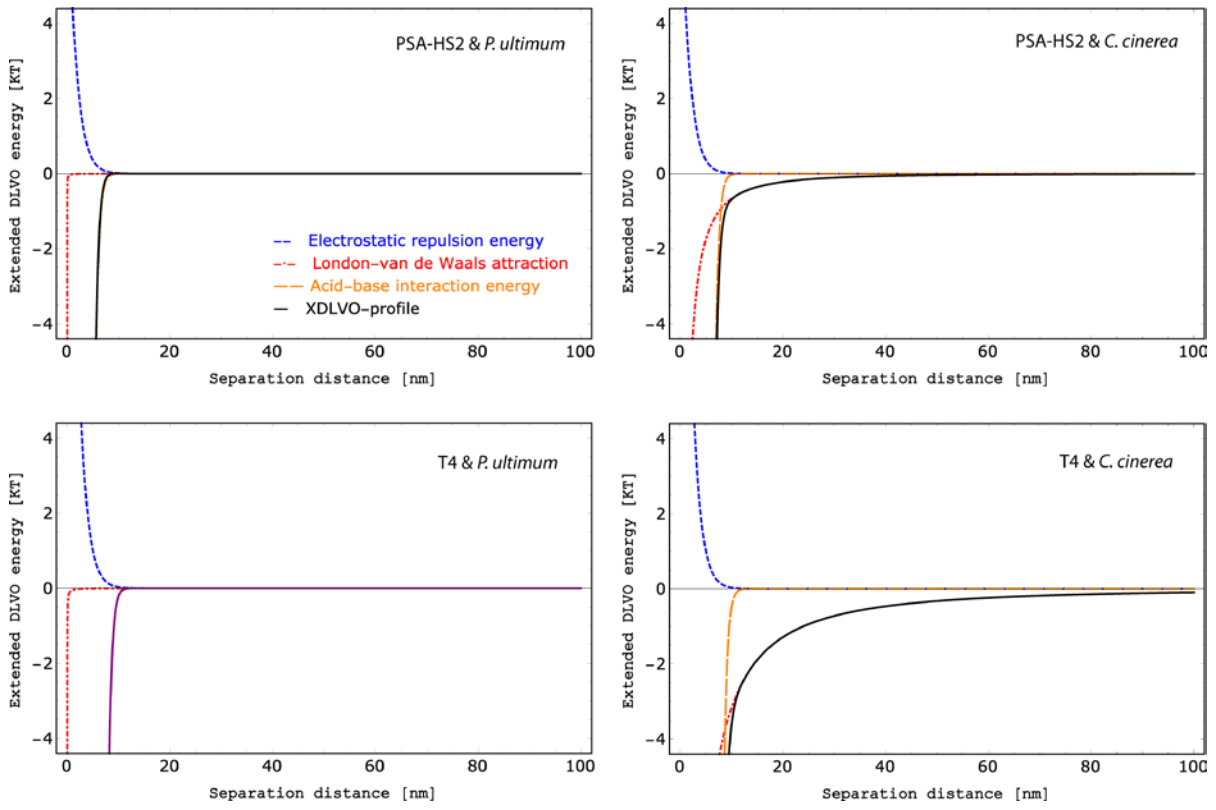
714

715

716

717

718



719

720

721 **Figure 4**

722

723